(Preprint) AAS 25-092

RVS® 3000-X LIDAR – POSE ESTIMATION – TEST RESULT VS LANDSAT7 MOCKUP

Lukas Kroßner[*], Christoph Schmitt[*], Tristan Röll[*], Eugene Skelton[†], Kevin H. Miller[†], , Michael Windmüller[*], Michael Schwarz[*], Max Möller[*]

The RVS® 3000-X from Jena-Optronik GmbH combines a high-resolution scanning LIDAR with robust image processing algorithms for autonomous rendezvous and docking. The generic design of the LIDAR utilizes all heritage and lessons learned from RVS® 3000, which has reached TRL9 during its maiden flight to the International Space Station in 2019 on Cygnus NG-11 as well as from RVS® 3000-3D, which enabled the first servicing of GEO satellites in frame of Mission Extension Vehicle (MEV) 1 in 2020 and MEV-2 in 2021 using model-based pose estimation.

So far, experience with concept of operations development for RVS® 3000-X has been gained for various Artemis docking targets, uncooperative satellites in debris removal missions and sample-return missions such as Mars Sample Return. Last but not least, concepts of operation for lunar landing missions are under consideration. It is state of the art that early concept of operations development is accompanied by test campaigns, which consolidate the performance and generate trust in the combination of the navigation sensor and the use case. Here we present test results of the RVS® 3000-X LIDAR system against a Landsat7 mockup. Thereby, we evaluate the RVS® 3000-X LIDAR system performance at key pillars of the envisioned concept of operation of the On-orbit Servicing, Assembly and Manufacturing 1 (OSAM-1) mission.

INTRODUCTION

Space-qualified LIDAR (Light detection and ranging) technology has matured to serve a variety of mission scenarios where relative guidance and navigation is needed [1]. Current applications are rendezvous and docking with the International Space Station (ISS) or the Lunar Gateway [2], imaging and pose estimation of geo-stationary satellites [3], and rendezvous and capture for the Mars sample return missions [4]. Further, space-qualified LIDAR technology is pushed to aid landing maneuvers on the moon [5], planets [6-8] and asteroids [9-10].

The LIDAR is typically asked to provide a precise, robust, flexible three-dimensional point cloud measurement of the object at high sample rate. For landing maneuvers, a measurement of the relative velocity is of strong interest in addition. The measured point cloud is then analyzed to the specific need of the relative guidance and navigation system during the mission. The detailed requirements against the point cloud measurement and the subsequent analysis of it depend on the capabilities of the LIDAR, the properties of the client (e.g., dimensions, shape, optical properties) as well as on the relative distance between the client vehicle and the servicer. To cope with this

[*] Jena-Optronik GmbH, Otto-Eppenstein-Straße 3, Germany.
[†] NASA Goddard Space Flight Center, Greenbelt, Maryland, USA

complexity, it is common incorporate the development of the concept of operations (ConOps) of the LIDAR closely into the design of the guidance and navigation system of the mission.

Here we consider the performance of the RVS® 3000-X [11] scanning LIDAR system against a mock-up of the Landsat 7 spacecraft. The goal is to prepare a LIDAR concept of operations for the guidance and navigation system of the On-orbit Servicing, Assembly and Manufacturing 1 (OSAM-1) mission [12]. To this end, we shortly introduce the RVS® 3000-X LIDAR system, present the test setup and the LIDAR ConOps, which are tested during the ground test. Our main point is to present point cloud measurements as well as point cloud analysis results from RVS® 3000-X LIDAR with a flight-like 1:1 scale mock-up of the end of Landsat 7 with a single solar panel.

RVS® 3000-X AND THE LANDSAT7 MOCK-UP

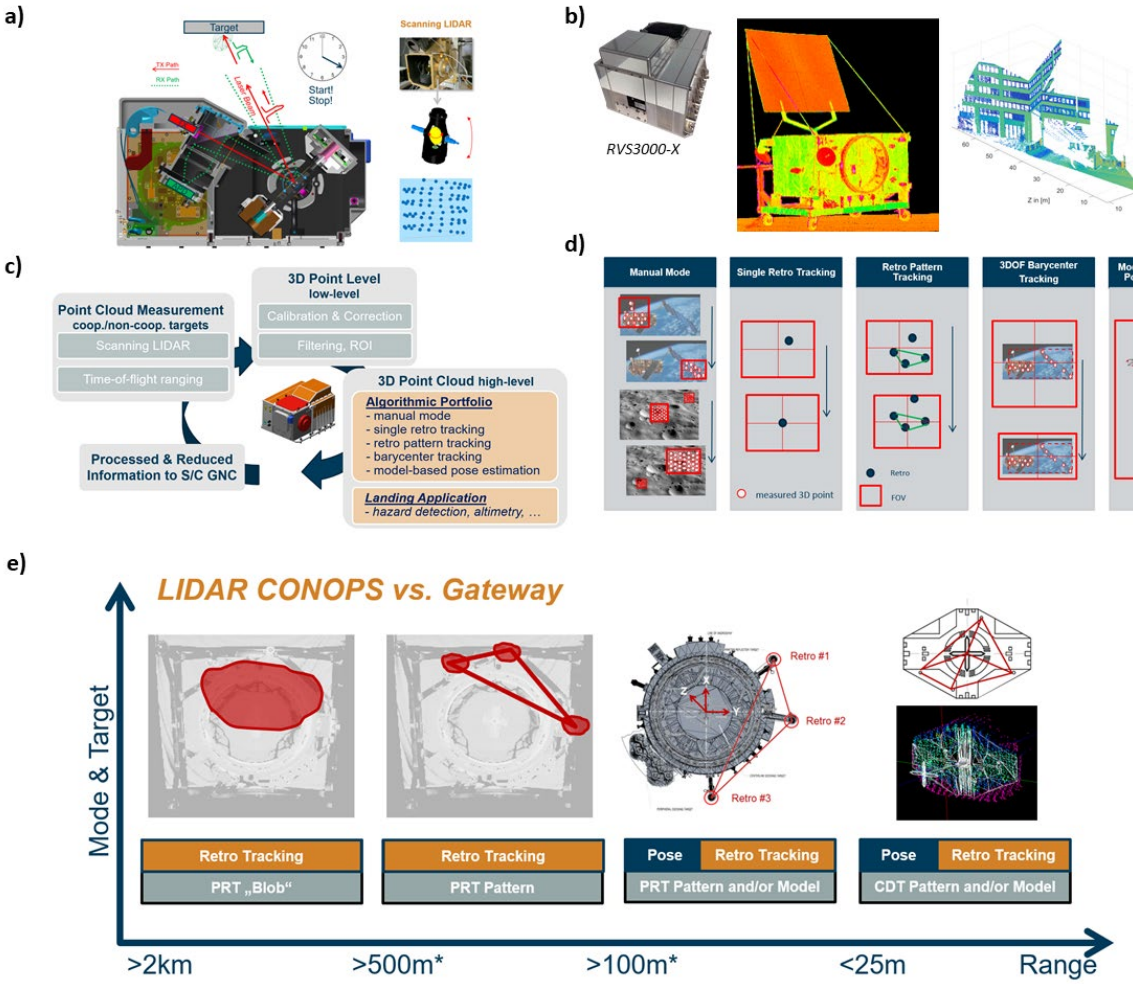

Figure 1. An illustration of the key aspects of the RVS® 3000 product family. a) Measurement of the 3D point cloud is enabled by time-of-flight measurement for the range and by high-performance angular measurement for azimuth and elevation. The gimbal scanning mechanism allows a flexible field of view, where consecutive laser shots are distributed along the scan pattern. b) A photograph of the RVS® 3000-X system (left). Examples od measured 3D point clouds with color-coded amplitude information (center) and a 3D

illustration (right). c) A functional breakdown of the RVS® 3000 product family. d) Various algorithmic options for point cloud analysis and e) example ConOps for an Artemis mission

Key aspects of the RVS® 3000-X LIDAR are illustrated in Figure 1. All system components of the RVS® 3000-X LIDAR, the laser, optics, detection electronics, scanner control and electronics for point cloud analysis are arranged in a single box. Figure 1 a) shows some illustration of the hardware design and Figure 1 c) a functional break down of RVS® 3000-X LIDAR. High-resolution point cloud measurement is achieved using time-of-flight measurement and a gimbal scanning mechanism. The detection electronics allows to measure the point cloud of an object simultaneously with some information about the intensity of the returning light pulse. See Figure 1 b) for an example of the point cloud left and an example of the measured information on amplitude in the center. The scanning LIDAR principle allows to provide a point cloud measurement, which can be flexibly optimized for the LIDAR ConOps along the mission. In this way, the point cloud measurement serves the subsequent point cloud analysis in an optimal way.

The RVS® 3000-X LIDAR provides several options for point cloud analysis. In Figure 1 d) an overview of possible modes for point cloud analysis is shown. For example, in case of so-called cooperative clients, the analysis often utilizes identification of retro-reflecting patterns on the client vehicle (e.g., for rendezvous with the International Space Station (ISS) or the Lunar Gateway). The retro-reflecting patterns are then used to provide 6 degree-of-freedom (6DOF) pose between servicer and the client vehicle. If there is a lack of fiducial markers on client vehicle, as for many in-orbit servicing scenarios of today, real-time 6DOF pose estimation can be achieved by matching the measured point cloud with a pre-known 3D model of the client vehicle, see Figure 1 d). For less geometrically complex objects, such as a sample container, a comparatively simple calculation of the barycenter of the point cloud maybe sufficient to fulfill the needs of the guidance and navigation system. Flexibility in the point cloud measurement and the point analysis are essential to serve a wide range of mission scenarios.

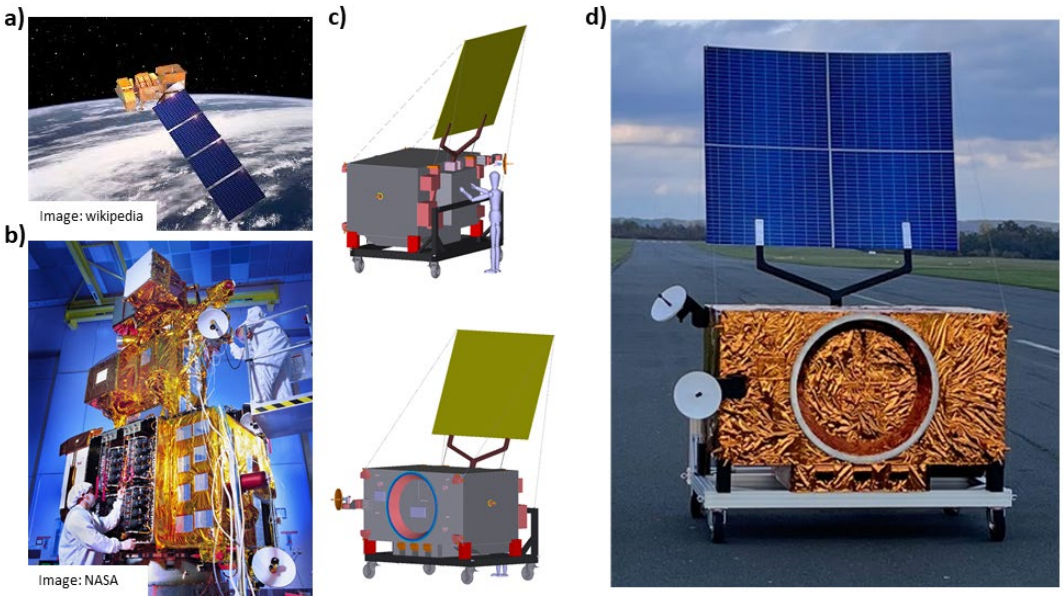

Figure 2. The 1:1 scale mock-up of the relevant part of the Landsat 7 satellite. a) An artistic view of the Landsat 7 satellite in space. b) Landsat 7 during its final integration. c) Top and bottom show a model of the Landsat 7 mock-up. A model of a man gives a reference for its size. s) shows the Landsat 7 mock-up on the run way of an airfield during the test campaign.

The information about how the LIDAR is operated along the mission is typically summarized in a ConOps. It contains information about the LIDAR operational parameters for point cloud measurement and the applied point cloud analysis strategy as function of range along the approach trajectory. An example for an Artemis mission is shown in Figure 1 e).

The LIDAR performance tests have been done using a 1:1 scale mock-up of the relevant part of the Landsat 7 satellite. For the mock-up, it is sufficient to consider the structure of the aft end and one of in total 4 solar panels of Landsat 7. Reduction of the mock-up to these parts of Landsat-7 is justified by feasibility of the test any by relevance for the approach trajectory, which is considered. The LIDAR ConOps during the mission will account for this by the chosen operational parameters of the LIDAR. Further, the mock-up has been designed and manufactured using materials, which are expected to resemble the optical properties of Landsat 7. This is important to ensure representativity between the LIDAR performance during ground testing and in space operation. However, the reachable representativity is sufficient but only limited. The information of the optical properties are estimates based on the used materials. The change of the optical properties during the ageing in space is not known. The design of the LIDAR ConOps shall account for some margins with respect to those aspects.

RELATIVE NAVIGATION – 3DOF AND 6 DOF POSE ESTIMATION

The LIDAR provides relative navigation and pose estimation as input to the guidance and navigation system of the spacecraft. Functionally, the RVS® 3000-X LIDAR measures a point cloud, which is then analyzed by its computational capabilities to provide (6DOF) pose between servicer and the client vehicle for example. Typically, the result of the analysis is delivered to the guidance and navigation system at an update rate of 2 Hz. In case of the test here, we match the measured point cloud with a pre-known three-dimensional model of the Landsat 7 mockup using the docking mode of RVS® 3000-X LIDAR. This is achieved using a dedicated image processing board, which strongly enhances image processing capabilities of RVS® 3000-X LIDAR.

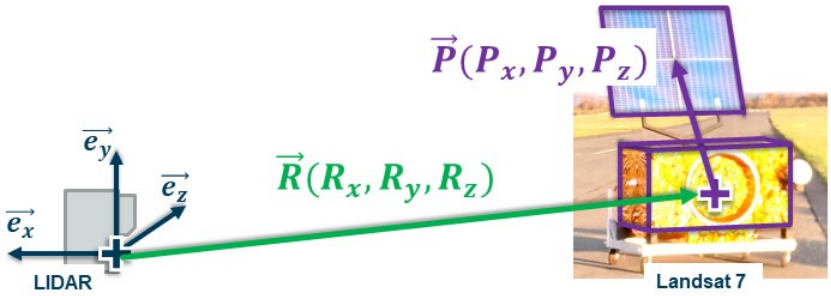

Figure 3. Relative navigation and pose estimation. The grey structure on the left indicates the LIDAR. The purple lines indicated the pre-known three-dimensional model, which is matched to the point cloud measurement. See text for detailed information on vector definitions.

Figure 3 illustrates relative navigation and pose estimation in the optical reference frame (ORF) of the RVS® 3000-X LIDAR. The ORF of the RVS® 3000-X LIDAR is marked by the unit vectors, $\vec{e_x}, \vec{e_y}, \vec{e_z}$. The vector $\vec{R}$ points from the origin of the optical reference frame to the Landsat 7 mockup. $\vec{R}$ gives the position, in other words, 3 degree of freedom pose (3DOF). In other words, it is the direction and distance from RVS® 3000-X to Landsat 7. The vector $\vec{P}$ is reached from the LIDAR line-of-sight, $\vec{L}$, in the ORF by a transformation, $\vec{P} = \vec{R} + M\vec{L}$, with M being a rotation matrix. M states the orientation of Landsat 7 with respect to LIDAR line-of-sight, $\vec{L}$. Both, $\vec{R}$ and M together are the 6 degree-of freedom pose estimation result of the point cloud analysis, which is

delivered to the guidance and navigation system of the servicer spacecraft typically at 2 Hz update rate.

TEST SETUP

The performed tests use Jena-Optronik's mobile LIDAR test facility. It consists of a van (see Figure 4 a), which is equipped with ground support equipment for operation of the RVS® 3000-X and a mobile turn table on which the RVS® 3000-X LIDAR can be operated (see Figure 4 c). The mockup is positioned on the runway of an airfield, which is sufficiently flat to allow for measurement distances up to 1200m (see Figure 4 e). Moving the van from one range-wise static position to another allows LIDAR performance measurements at various ranges. The combination of range with the turn table enables measurements where expected rotational motions from the spacecraft can be incorporated. So far, the rotational motion of the turn table is limited to LIDAR azimuth and elevation direction. Actively, moving the target or the van and operation of the turn table and RVS® 3000-X LIDAR allows the test to mimic spacecraft dynamics while LIDAR measurements are taken. In this way, many aspects of the rendezvous maneuver between servicer and client can be tested.

The LIDAR performance is characterized by comparison to "ground truth". "Ground truth" is a high-accuracy, high-precision measurement of the relative position and orientation of the Landsat 7 mockup in the LIDAR ORF. High-accuracy and high-precision is achieved by the usage of a coordinate measurement machine (CMM), ZEISS PRISMO, a LEICA workstation, see Figure 4 b), and a chain of fiducial markers (see Figure 4 c and see Figure 4 d). Both the CMM and the LEICA workstation are more accurate and precise than RVS® 3000-X while its measurement rate is much slower than RVS® 3000-X. The chain of fiducial markers enables the CMM and the LEICA to determine the following transformations between coordinate frames, from RVS® 3000-X ORF to RVS® 3000-X mechanical reference frame, from RVS® 3000-X mechanical reference frame to "van reference frame", see Figure 4 c), and from "van reference frame" to "Landsat 7 mockup reference frame", see Figure 4 d). The fiducial marker on the mockup can be covered such that it is not noted by the RVS® 3000-X.

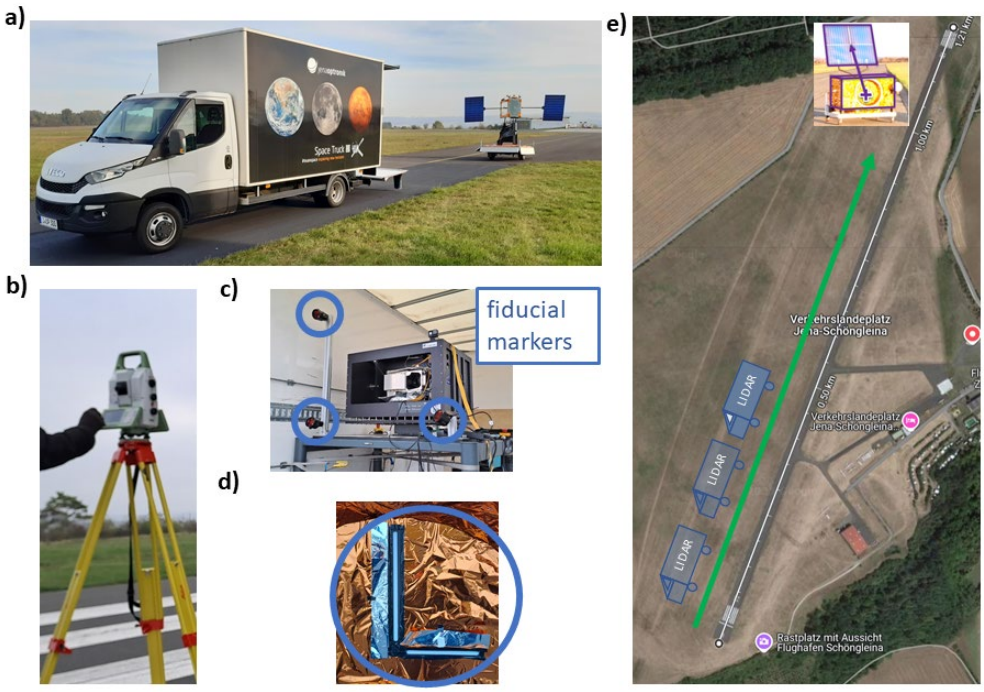

Figure 4. The test setup including equipment for "ground truth" measurement. a) shows JOP's Jena-Optronik's mobile LIDAR test facility for long range testing, b) shows the LEICA workstation. c) and d) are photographs of the fiducial markers, which needed to enable high-accuracy and high-precision "ground truth" determination. e) gives an impression of the setup on the airfield. Ranges up to 1400m can be tested.

RVS® 3000-X CONCEPT OF OPERATION AND TEST RESULTS

The long-range tests have the intent to evaluate the RVS® 3000-X performance at key pillars of the LIDAR ConOps during the mission. We limit ourselves to the presentation of static test results and 6DOF docking only.

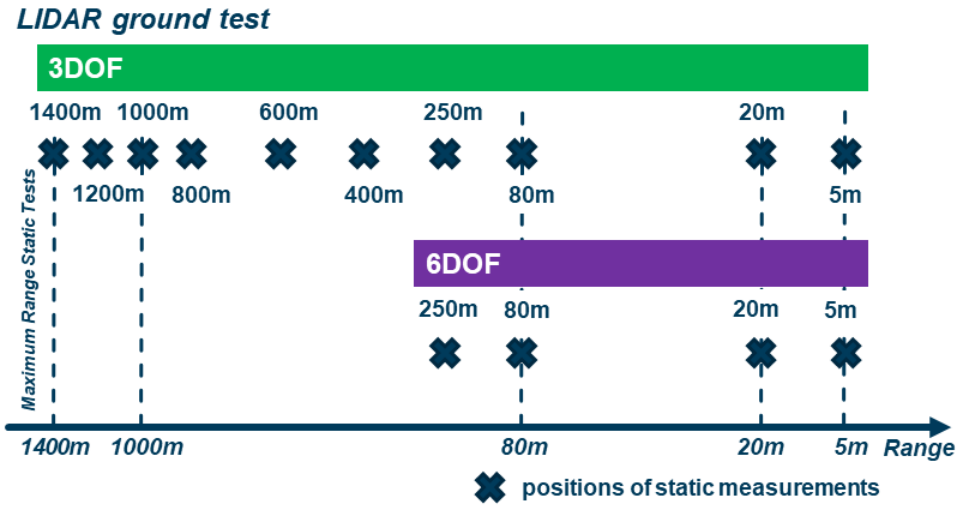

Figure 5. Tested RVS® 3000-X ConOps for a rendezvous and docking maneuver with Landsat7, see text for details.

A possible ConOps for the RVS® 3000-X along a rendezvous and docking maneuver with Landsat7 using RVS® 3000-X is shown in Figure 5. It shows the range between RVS® 3000-X and the Landsat 7 mockup at the bottom. Crosses mark the range values at which static tests have been performed. In the example, at long ranges, between 1400m and 250m 3DOF relative navigation by the RVS® 3000-X "retro manual mode" is used primarily. To reach optimized RVS® 3000-X performance, the operational parameters RVS® 3000-X for point cloud measurement and point cloud analysis have been optimized over range. 6DOF pose estimation maybe used from 250m on towards smaller ranges using the "docking mode" of RVS® 3000-X for point cloud analysis. The measured point cloud is matched with a pre-known 3D model in the RVS® 3000-X "docking mode" such that 6DOF pose can be provided.

Before we turn to evaluation of 6DOF performance by comparison to the "ground truth", we illustrate the data quality in Figure 6 for a few examples. At some range positions, two different orientations, 0° and 45°, between mockup and RVS® 3000-X have been measured. These are shown in Figure 6. High-resolution measurements are in the top part and measurements in docking mode is in the bottom part. Considering a number of orientations between mockup and LIDAR illustrates the sensitivity of RVS® 3000-X with respect to the mockup's optical properties. Changing the orientation of the mock-up has impact on the intensity of the light, which returns to the LIDAR. If the 6DOF performance is the similar for 0° and 45° orientation, robustness of the point cloud measurement and analysis is demonstrated. Our measurements of 6DOF performance at different orientations for demonstrates robustness with the variability in mock-up optical properties, mock-up features and variability in the approach trajectory.

Another interesting observation in Figure 6 is the behavior of the point cloud at longer ranges, 800m and 250m. It becomes "less sharp" for high-resolution measurements in docking configurations compared to the point cloud appearance at smaller ranges. The observation can be attributed to the divergence of the laser beam. At large range, the size of the laser beam reaches the size of relevant structures of the mockup such that an averaging effect of the range measurement over the mock-up structures leads to a "less sharp" point cloud.

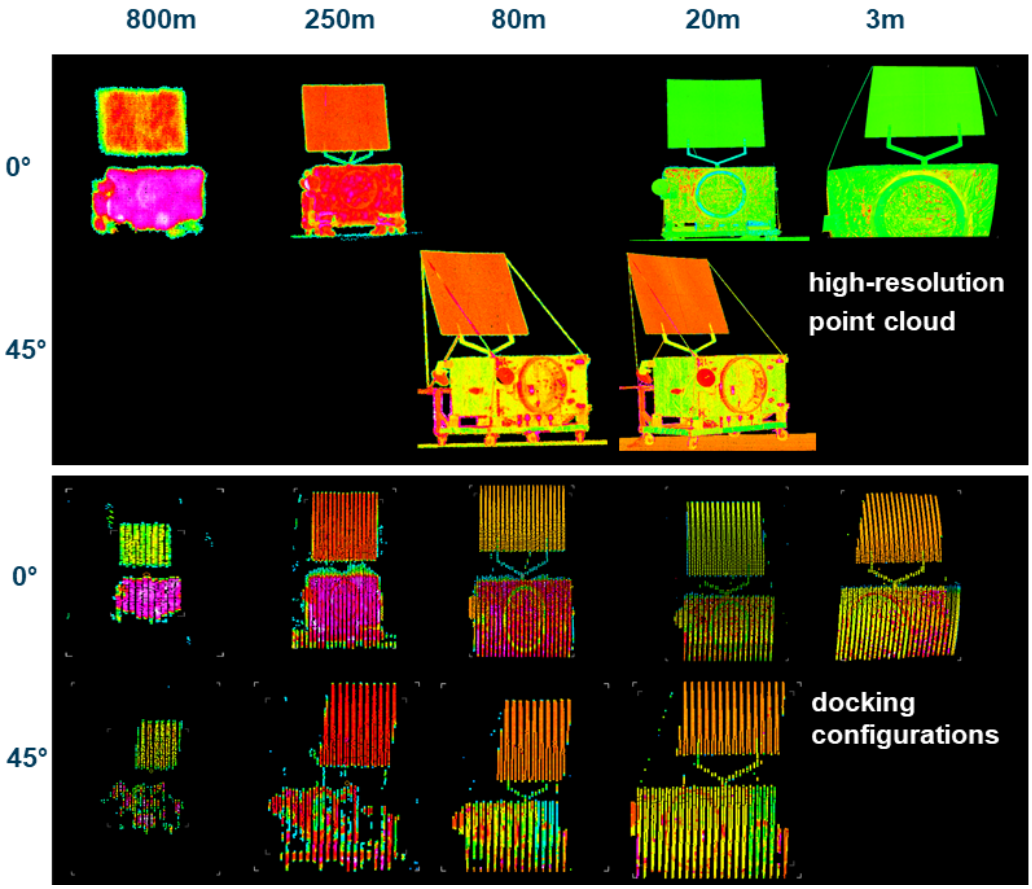

Figure 6. Illustration of data quality. First and second row from the top show high-resolution point cloud measurements of the mockup for two different orientations, close to 0° and close to 45°. Third and fourth row from the top show that point cloud as it is measured by RVS® 3000-X in the respective distance. In all cases, the amplitude of the returning light is color coded. The range reduces with the column, from left to right, see the label at the top.

Last but not least, we show the noise and bias of RVS® 3000-X 6DOF pose estimation results with respect to the "ground truth" measurement in Figure 7. Bias and noise values for position and orientation are determined based on comparison between RVS®3000-X and the "ground truth". Approximately fifty collections of 2Hz up and down scans of RVS®3000-X are considered. Further, results from all orientations, 0° and 45° are shown. The top row, a) and b), shows bias and noise for position for each of the vector component. The bottom row shows bias and noise for the orientation around the indicated axis.

The noise (Figure 7 b) and d)), which increases with range for position and orientation, can be understood by considering that the exact sampling of 3D points on the mock-up by RVS®3000-X varies slightly from 2Hz scan to 2Hz scan. The slight variation is caused by the LIDAR internal timing between motion of the scanner and firing of the laser pulses, see the stripe-like features in Figure°6, which stem from the scanner's elevations motion in Figure 6. It increases with the range as the scanner motion and laser firing rate is kept the same for all ranges such that the number of 3D measurement actually decrease with range. Combining this thought, with the stripe-like structure explains the increasing noise for increasing range. A similar explanation might be considered for the range dependence of position bias. The orientation bias shows a roughly constant value with range, see Figure 7 b). We attribute this observation to deviations between the actual geometry of

the actual mock-up and the reference model which is used for 6DOF pose estimation. A few degrees deviation for the extended solar panel is beyond the accuracy of the mock-up manufacturing. In total, the presented test results for determined bias and noise values for position and orientation based on the draft ConOps for RVS®3000-X against Landsat 7 demonstrate in family performance to the high TRL-9 product line.

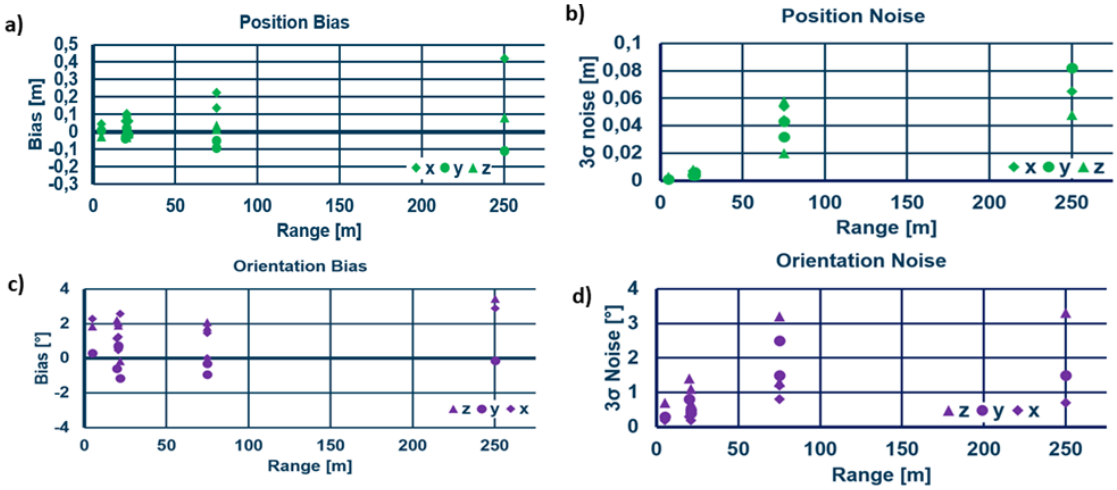

Figure 7. Noise and bias of 6DOF pose estimation in RVS® 3000-X docking mode. a) and b) show position bias and noise for the position measurement using RVS® 3000-X docking mode with the respective configuration. c) and d) show the same, for the measurement of the Landsat 7 orientation.

CONCLUSION

The RVS®3000-X LIDAR performance has been tested against a Landsat 7 mockup with focus on 6DOF pose estimation performance. The test has been performed using Jena-Optronik's long-range test facility including "ground truth" determination. The measurement results show very good data quality and bias and noise values for position and orientation from the RVS®3000-X LIDAR docking mode, which are in-family with the high TRL9 product line. Thus, the test results of RVS®3000-X LIDAR against Landsat 7 demonstrate feasibility of robust inputs of LIDAR measurements to the guidance and navigation system during a rendezvous and docking maneuver.

REFERENCES

[1] C. Schmitt et al. RVS®3000-X LIDAR – Applications from Docking to Sample Return and Lunar Landing AAS Guidance, Navigation and Control (GN&C) Conference, Breckenridge 2024

[2] C. Schmitt et al. RVS®3000-X LIDAR – Design and Test Results For the Example of Artemis Rendezvous AAS Guidance, Navigation and Control (GN&C) Conference, Breckenridge 2023

[3] C. Schmitt et al. RVS®3000-3D LIDAR – 3D imaging and Pose Estimation during first GEO Satellite Servicing AAS Guidance, Navigation and Control (GN&C) Conference, Breckenridge 2021

[4] Keyvan Kanani et al. MSR-ERO Rendezvous Navigation Sensors and Image Processing ESA Conference on Guidance, Navigation & Control Systems (GNC), Sopot, 2023

[5] T. Kämpfe et al. RVS®3000 LIDAR Product Family from Rendezvous and Docking Applications to Hazard Mapping for Planetary Landing ESA Conference on Guidance, Navigation & Control Systems (GNC), Sopot, 2023

[6] Xiao, Xueming, Meibao Yao, Hutao Cui, and Yuegang Fu. "Safe Mars Landing Strategy: Towards Lidar-Based High Altitude Hazard Detection." Advances in Space Research 63, no. 8 (April 15, 2019): 2535–50. https://doi.org/10.1016/j.asr.2019.01.005.

[7] Knicely, Joshua J. C., Martha S. Gilmore, Richard J. Lynch, and Robert R. Herrick. “Strategies for Safely Landing on Venusian Tesserae.” Planetary and Space Science 228 (April 1, 2023): 105652. https://doi.org/10.1016/j.pss.2023.105652.
[8] Punjiya, Meera, Kevin Ryu, Brian Aull, K. Alexander McIntosh, Kevan Donlon, Mike Brattain, Hermanus Pretorius, Denis Nothern, Noah Pestana, and Thomas Karolyshyn. “A Direct-Detection LIDAR Detector for the Europa Lander Concept.” In Advanced Photon Counting Techniques XVI, 12089:8–17. SPIE, 2022.
[9] Hofacker, Max, Harvey Gomez Martinez, Martin Seidl, Fran Domazetovic, Larissa Balestrero Machado, Thomas Pany, and Roger Förstner. “LiDAR-Based Autonomous Landing on Asteroids: Algorithms, Prototyping and End-to-End Testing with a UAV-Based Satellite Emulator.” In 2023 IEEE/ION Position, Location and Navigation Symposium (PLANS), 1293–1302, 2023.
[10] Carson, J. et al., “Precise and Safe Landing Navigation Technologies for Solar System Exploration” Planetary Science and Astrobiology Decadal Survey 53 (May 1, 2021): 413. https://doi.org/10.3847/25c2cfeb.7f40f610.
[11] Jena-Optronik RVS®3000 and RVS3000®3000-X LIDAR Product Family Datasheet
[12] https://www.nasa.gov/mission/on-orbit-servicing-assembly-and-manufacturing-1/